Pramana – J. Phys. (2016) 87: 40
DOI 10.1007/s12043-016-1252-4

Scalar sector of two-Higgs-doublet models: A minireview

GAUTAM BHATTACHARYYA* and DIPANKAR DAS

Saha Institute of Nuclear Physics, 1/AF Bidhan Nagar, Kolkata 700 064, India
*Corresponding author. E-mail: gautam.bhattacharyya@saha.ac.in

Published online 24 August 2016

Abstract. A vast literature on the theory and phenomenology of two-Higgs-doublet models (2HDM) exists since long. However, the present situation demands a revisit of some 2HDM properties. Now that a 125 GeV scalar resonance has been discovered at the LHC, with its couplings to other particles showing increasing affinity to the Standard Model Higgs-like behaviour, the 2HDM parameter space is more squeezed than ever. We briefly review the different parametrizations of the 2HDM potential and discuss the constraints on the parameter space arising from the unitarity and stability of the potential together with constraints from the oblique electroweak T-parameter. We also differentiate the consequences of imposing a global continuous $U(1)$ symmetry on the potential from a discrete Z_2 symmetry.

Keywords. Higgs; beyond Standard Model; two-Higgs doublet.

PACS Nos 12.60.−i; 12.60.Fr; 14.80.Ec

1. Introduction

The discovery of a new boson in July 2012 by the ATLAS [1] and CMS Collaborations [2] of the CERN Large Hadron Collider (LHC) is undoubtedly the greatest achievement of this decade in the field of Particle Physics. This is *most likely* 'the' Higgs boson [3–7], the so far eluding final missing piece of the Standard Model (SM). But the SM has certain inadequacies. For example, it cannot account for observations like neutrino oscillations and dark matter. It cannot also provide adequate matter–antimatter asymmetry of the Universe. These constitute the primary motivation to look for avenues beyond the SM, which we often call BSM scenarios. The SM relies on the minimal choice of a single $SU(2)$ scalar doublet acquiring a vacuum expectation value (VEV) for giving masses to all the particles (except the neutrino) contained in the SM. One natural direction towards constructing BSM scenarios is to extend the SM scalar sector. In doing so, one may run into the risk of altering the tree-level value of the precisely measured oblique electroweak parameter ρ (or, equivalently T). If we construct an $SU(2) \times U(1)$ gauge theory with N number of scalar multiplets, then the general expression for the tree-level ρ-parameter is [8]

$$\rho^{\text{tree}} = \frac{\sum_{i=1}^{N} \left\{ T_i(T_i+1) - (Y_i^2/4) \right\} v_i}{\frac{1}{2}\sum_{i=1}^{N} Y_i^2 v_i}, \tag{1}$$

where T_i and Y_i denote the weak isospin and hypercharge of the ith scalar multiplet respectively, and v_i is the VEV acquired by the neutral component of that multiplet. It is easy to verify that if the scalar sector contains only $SU(2)$ singlets ($T_i = 0$) and doublets ($T_i = 1/2$) with $Y_i = 0$ and ± 1 respectively, then $\rho^{\text{tree}} = 1$ is automatically satisfied without requiring any fine-tuning among the VEVs. This conforms to the experimental value of ρ, which is very close to unity [9]. In this article we restrict our discussions to the doublet extensions only. The simplest extension of this type is two-Higgs-doublet model (2HDM) [10], which has received a lot of attention mainly because minimal supersymmetry relies on it. 2HDM scenarios have also been investigated to look for additional sources of CP violation for generating baryon asymmetry of the Universe of sufficient size [11]. In a general 2HDM, both the scalar doublets, which we call Φ_1 and Φ_2, can couple to fermions of both types with $T_3 = 1/2$ (up-type) and $-1/2$ (down-type). The up- and down-type Yukawa matrices are not, in general, simultaneously diagonalizable. This will introduce flavour changing neutral currents (FCNC) mediated by the

neutral scalars at tree-level. It was shown by Glashow and Weinberg [12], and independently by Paschos [13], that such tree-level FCNC can be avoided if fermions of a particular electric charge receive their masses from a single scalar doublet. This prescription can be realized by introducing a discrete or a continuous symmetry that apply on the scalars Φ_1 and Φ_2 as well as on the fermions. Under the discrete symmetry, one of the scalars is even ($\Phi_2 \to \Phi_2$) and the other is odd ($\Phi_1 \to -\Phi_1$). There are four different possibilities for assigning Z_2 parities to the fermions which can avoid tree-level FCNCs, i.e. ensure natural flavour conservation, so that Glashow–Weinberg–Pashcos theorem holds true. These correspond to the following four types of 2HDMs:

(i) Type I: All quarks and leptons couple to only one scalar doublet Φ_2.
(ii) Type II: Φ_2 couples to up-type quarks, while Φ_1 couples to down-type quarks and charged leptons (minimal supersymmetry conforms to this category).
(iii) Type X (or 'lepton-specific'): Φ_2 couples to all quarks, while Φ_1 couples to all leptons.
(iv) Type Y (or 'flipped'): Φ_2 couples to up-type quarks and leptons, while Φ_1 couples to down-type quarks.

There is also the option for preventing tree-level FCNC by assuming the up- and down-type Yukawa matrices to be proportional to each other [14]. However, the radiative stability of the absence of FCNC couplings in these models is not guaranteed [15]. The Branco–Grimus–Lavoura (BGL) model [16] does on the other hand admit tree-level FCNC couplings. But those couplings are related to the off-diagonal entries of the Cabibbo–Kobayashi–Maskawa (CKM) matrix and are naturally suppressed. The phenomenology of the BGL scenario has been studied in detail in refs [17,18]. A conceptually similar idea for suppressing FCNC with discrete symmetries was pursued in [19]. In this article, we shall not elaborate any further on the FCNC issues, as we shall not discuss the Yukawa sector of 2HDM.

In the subsequent sections, we analyse the scalar potential, identify the physical scalar eigenstates and reach the limit in which one physical scalar resembles the 125 GeV Higgs boson. For simplicity, we assume all the parameters in the potential to be real so that CP is manifestly conserved in the scalar sector. For discussions on CP violation in 2HDM scalar sector we refer the reader to refs [20–22], where conditions for CP violation/conservation have been diagnosed in detail. With these assumption, we derive the relations among the parameters of the potential that need to be satisfied to ensure that the potential is stable, i.e. it is bounded from below, at the weak scale. We then derive the constraints arising from the requirement of unitarity by studying the scattering amplitudes of $2 \to 2$ states involving the scalars and the gauge bosons. After that, we combine the stability and unitarity constraints to impose numerical constraints on the physical scalar masses and other parameters. Now that one scalar has been observed around 125 GeV, constraints on the remaining parameter space have become more stringent. We conclude by highlighting some salient features that arise from the above considerations.

2. The scalar potential

There are two equivalent notations that are used in the literature to write the 2HDM scalar potential with a softly broken Z_2 symmetry ($\Phi_1 \to \Phi_1$, $\Phi_2 \to -\Phi_2$):

Parametrization 1:

$$\begin{aligned} V(\Phi_1, \Phi_2) = {} & m_{11}^2 \Phi_1^\dagger \Phi_1 + m_{22}^2 \Phi_2^\dagger \Phi_2 \\ & - (m_{12}^2 \Phi_1^\dagger \Phi_2 + \text{h.c.}) + \frac{\beta_1}{2} (\Phi_1^\dagger \Phi_1)^2 \\ & + \frac{\beta_2}{2} (\Phi_2^\dagger \Phi_2)^2 + \beta_3 (\Phi_1^\dagger \Phi_1)(\Phi_2^\dagger \Phi_2) \\ & + \beta_4 (\Phi_1^\dagger \Phi_2)(\Phi_2^\dagger \Phi_1) \\ & + \left\{ \frac{\beta_5}{2} (\Phi_1^\dagger \Phi_2)^2 + \text{h.c.} \right\}. \end{aligned} \tag{2}$$

Parametrization 2:

$$\begin{aligned} V = {} & \lambda_1 \left(\Phi_1^\dagger \Phi_1 - \frac{v_1^2}{2} \right)^2 + \lambda_2 \left(\Phi_2^\dagger \Phi_2 - \frac{v_2^2}{2} \right)^2 \\ & + \lambda_3 \left(\Phi_1^\dagger \Phi_1 + \Phi_2^\dagger \Phi_2 - \frac{v_1^2 + v_2^2}{2} \right)^2 \\ & + \lambda_4 ((\Phi_1^\dagger \Phi_1)(\Phi_2^\dagger \Phi_2) - (\Phi_1^\dagger \Phi_2)(\Phi_2^\dagger \Phi_1)) \\ & + \lambda_5 \left(\text{Re}\, \Phi_1^\dagger \Phi_2 - \frac{v_1 v_2}{2} \right)^2 + \lambda_6 \left(\text{Im}\, \Phi_1^\dagger \Phi_2 \right)^2. \end{aligned} \tag{3}$$

The bilinear terms proportional to m_{12}^2 in eq. (2) or λ_5 in eq. (3) break the Z_2 symmetry softly. The presence of these soft breaking terms has implications in ensuring decoupling behaviour of these models (briefly discussed in the concluding section). Note that when we minimize the potential of eq. (2), the two minimization conditions can be used to trade m_{11}^2 and m_{22}^2 for v_1 and v_2 and the potential can be cast in the form of eq. (3).

The connections between the parameters of eqs (2) and (3) are given below:

$$m_{11}^2 = -(\lambda_1 v_1^2 + \lambda_3 v^2); \quad m_{22}^2 = -(\lambda_2 v_2^2 + \lambda_3 v^2);$$
$$m_{12}^2 = \frac{\lambda_5}{2} v_1 v_2; \qquad \beta_1 = 2(\lambda_1 + \lambda_3);$$
$$\beta_2 = 2(\lambda_2 + \lambda_3); \qquad \beta_3 = 2\lambda_3 + \lambda_4;$$
$$\beta_4 = \frac{\lambda_5 + \lambda_6}{2} - \lambda_4; \qquad \beta_5 = \frac{\lambda_5 - \lambda_6}{2}. \tag{4}$$

In eq. (4), $v = \sqrt{v_1^2 + v_2^2} = 246$ GeV, where v_1 and v_2 are the VEVs of the two doublets Φ_1 and Φ_2 respectively. For most of this article, we choose to work with the notation of eq. (3).

Before we proceed further, we comment on the relative status of the two parametrizations of the potential. The structure in 'Parametrization 1' is more general than that in 'Parametrization 2'. It is possible to go from '1' to '2' but not the other way. In the second one it has been assumed that both scalars receive VEVs, while for the first this need not be the case. So the inert doublet scenario can be realized only in the first parametrization, e.g. in a simple illustrative scenario, when the dimensionless couplings $\beta_2 = \beta_3 = \beta_4 = \beta_5 = 0$, the mass mixing parameter $m_{12}^2 = 0$ and $m_{22}^2 > 0$. Then the second Higgs doublet Φ_2 does not acquire any VEV, and the SM scalar potential is recovered with the relation $v^2 = v_1^2 = -m_{11}^2/\beta_1$. On the other hand, if both doublets do indeed get VEVs, there is a correspondence between the parameters in the two cases, which we have explicitly written down in eq. (4).

2.1 *Physical eigenstates*

We express the scalar doublets as

$$\Phi_i = \frac{1}{\sqrt{2}} \begin{pmatrix} \sqrt{2} w_i^+ \\ (h_i + v_i) + i z_i \end{pmatrix}. \tag{5}$$

Then we construct the mass matrices using eq. (3). As we have assumed all the potential parameters to be real, there will be no bilinear mixing term of the form $h_i z_j$. As a result, the neutral mass eigenstates will also be the eigenstates of CP. For the charged sector we get the following mass matrix:

$$V_{\text{mass}}^{\text{charged}} = \begin{pmatrix} w_1^+ & w_2^+ \end{pmatrix} M_C^2 \begin{pmatrix} w_1^- \\ w_2^- \end{pmatrix},$$

with

$$M_C^2 = \frac{\lambda_4}{2} \begin{pmatrix} v_2^2 & -v_1 v_2 \\ -v_1 v_2 & v_1^2 \end{pmatrix}. \tag{6}$$

Diagonalizing M_C^2 we obtain a physical charged Higgs pair ($H^\pm$) and a pair of charged Goldstones ($\omega^\pm$) as follows:

$$\begin{pmatrix} \omega^\pm \\ H^\pm \end{pmatrix} = \begin{pmatrix} \cos\beta & \sin\beta \\ -\sin\beta & \cos\beta \end{pmatrix} \begin{pmatrix} w_1^\pm \\ w_2^\pm \end{pmatrix}, \tag{7}$$

where $\tan\beta = v_2/v_1$. The mass of the charged Higgs pair ($H^\pm$) is found to be

$$m_{H^+}^2 = \frac{\lambda_4}{2} v^2. \tag{8}$$

Similarly, for the pseudoscalar part one can easily find

$$V_{\text{mass}}^{\text{CP-odd}} = \begin{pmatrix} z_1 & z_2 \end{pmatrix} \frac{1}{2} M_P^2 \begin{pmatrix} z_1 \\ z_2 \end{pmatrix},$$

with

$$M_P^2 = \frac{\lambda_6}{2} \begin{pmatrix} v_2^2 & -v_1 v_2 \\ -v_1 v_2 & v_1^2 \end{pmatrix}. \tag{9}$$

The diagonalization in CP-odd sector is similar to that in the charged sector. Here we shall get a physical pseudoscalar (A) and a neutral Goldstone (ζ) as follows:

$$\begin{pmatrix} \zeta \\ A \end{pmatrix} = \begin{pmatrix} \cos\beta & \sin\beta \\ -\sin\beta & \cos\beta \end{pmatrix} \begin{pmatrix} z_1 \\ z_2 \end{pmatrix}. \tag{10}$$

The mass of the pseudoscalar is given by

$$m_A^2 = \frac{\lambda_6}{2} v^2. \tag{11}$$

For the CP-even scalar part we find

$$V_{\text{mass}}^{\text{CP-even}} = \begin{pmatrix} h_1 & h_2 \end{pmatrix} \frac{1}{2} M_S^2 \begin{pmatrix} h_1 \\ h_2 \end{pmatrix},$$

with

$$M_S^2 = \begin{pmatrix} A_S & B_S \\ B_S & C_S \end{pmatrix}, \tag{12a}$$

where

$$A_S = 2(\lambda_1 + \lambda_3) v_1^2 + \frac{\lambda_5}{2} v_2^2, \tag{12b}$$

$$B_S = 2\left(\lambda_3 + \frac{\lambda_5}{4}\right) v_1 v_2, \tag{12c}$$

$$C_S = 2(\lambda_2 + \lambda_3) v_2^2 + \frac{\lambda_5}{2} v_1^2. \tag{12d}$$

The masses of the physical eigenstates, H (heavier) and h (lighter), can be readily obtained as

$$m_H^2 = \frac{1}{2}\left[(A_S + C_S) + \sqrt{(A_S - C_S)^2 + B_S^2}\right], \tag{13a}$$

$$m_h^2 = \frac{1}{2}\left[(A_S + C_S) - \sqrt{(A_S - C_S)^2 + B_S^2}\right]. \tag{13b}$$

The physical scalars are obtained by rotating the original basis by an angle α:

$$\begin{pmatrix} H \\ h \end{pmatrix} = \begin{pmatrix} \cos\alpha & \sin\alpha \\ -\sin\alpha & \cos\alpha \end{pmatrix} \begin{pmatrix} h_1 \\ h_2 \end{pmatrix}. \tag{14}$$

This rotation angle is defined through the following relation:

$$\tan 2\alpha = \frac{2B_S}{A_S - C_S} = \frac{2(\lambda_3 + (\lambda_5/4))\, v_1 v_2}{\lambda_1 v_1^2 - \lambda_2 v_2^2 + (\lambda_3 + (\lambda_5/4))(v_1^2 - v_2^2)}. \tag{15}$$

Note that there were eight parameters to start with: v_1, v_2 and six lambdas. We trade v_1 and v_2 for v and $\tan\beta$. All the lambdas except λ_5 can be traded for four physical scalar masses and α. The relations between these two equivalent sets of parameters are given below:

$$\lambda_1 = \frac{1}{2v^2\cos^2\beta}\left[m_H^2\cos^2\alpha + m_h^2\sin^2\alpha - \frac{\sin\alpha\cos\alpha}{\tan\beta}(m_H^2 - m_h^2)\right] - \frac{\lambda_5}{4}(\tan^2\beta - 1), \tag{16a}$$

$$\lambda_2 = \frac{1}{2v^2\sin^2\beta}\left[m_h^2\cos^2\alpha + m_H^2\sin^2\alpha - \sin\alpha\cos\alpha\tan\beta\left(m_H^2 - m_h^2\right)\right] - \frac{\lambda_5}{4}(\cot^2\beta - 1), \tag{16b}$$

$$\lambda_3 = \frac{1}{2v^2}\frac{\sin\alpha\cos\alpha}{\sin\beta\cos\beta}(m_H^2 - m_h^2) - \frac{\lambda_5}{4}, \tag{16c}$$

$$\lambda_4 = \frac{2}{v^2}m_{H^+}^2, \tag{16d}$$

$$\lambda_6 = \frac{2}{v^2}m_A^2. \tag{16e}$$

Among these, v is already known (246 GeV) and if we assume that the lightest CP-even Higgs is what has been observed at the LHC, then m_h is also known (125 GeV). The rest of the parameters need to be constrained from theoretical as well as experimental considerations.

2.2 *The alignment limit*

The alignment limit corresponds to recovering a CP-even scalar mass eigenstate with exactly the same gauge, Yukawa and self-couplings at tree-level as those of the SM Higgs bosons. To start with, it is instructive to look at the trilinear gauge-Higgs couplings which stem from the Higgs kinetic terms:

$$\mathscr{L}_{\text{kin}}^{\text{scalar}} = |D_\mu\Phi_1|^2 + |D_\mu\Phi_2|^2 \ni \frac{g^2}{2}W_\mu^+ W^{\mu-}(v_1h_1 + v_2h_2). \tag{17}$$

Clearly, the combination

$$H^0 = \frac{1}{v}(v_1h_1 + v_2h_2) \tag{18}$$

will have gauge couplings exactly as the SM Higgs boson and its orthogonal combination (R) will not have any RZZ or RWW trilinear couplings. H^0 also mimics the SM Higgs in Yukawa couplings. The states H^0 and R can be obtained by applying the same rotation as in the charged and pseudoscalar sectors:

$$\begin{pmatrix} H^0 \\ R \end{pmatrix} = \begin{pmatrix} \cos\beta & \sin\beta \\ -\sin\beta & \cos\beta \end{pmatrix} \begin{pmatrix} h_1 \\ h_2 \end{pmatrix}. \tag{19}$$

Note that this SM-like state H^0 is not guaranteed to be a mass eigenstate in general. The alignment limit specifically implies the condition under which H^0 coincides with one of the CP-even physical eigenstates. To go to the physical basis (H, h) from (H^0, R) one needs the following rotation:

$$H = \cos(\beta-\alpha)H^0 - \sin(\beta-\alpha)R, \tag{20a}$$

$$h = \sin(\beta-\alpha)H^0 + \cos(\beta-\alpha)R. \tag{20b}$$

Clearly, if we want the lightest CP-even scalar h to posses SM-like couplings, we must set $\sin(\beta-\alpha) = 1$, which is the definition of the alignment limit. Thus, by going to this limit, one more parameter is reduced.

Now we come to the important question of how crucial the alignment limit is in the context of current LHC Higgs data. Many global fit results in view of the recent data can be found in [23–28]. In figure 1 we display the results of a recent analysis [23]. The orange part represents the 95% CL allowed region from measurements of the Higgs signal strengths in various channels (for the latter, see figure 2). As the data are compatible with the SM predictions, the alignment limit is preferred. The horizontal widths of the allowed regions reflect the present accuracy of measurements. In ref. [28], it has been shown how this width will shrink if future measurements continue to agree more with the SM predictions with greater accuracy, thus pushing us closer to the alignment limit. The SM alignment limit has also been motivated by employing different global symmetries of the scalar potential [29].

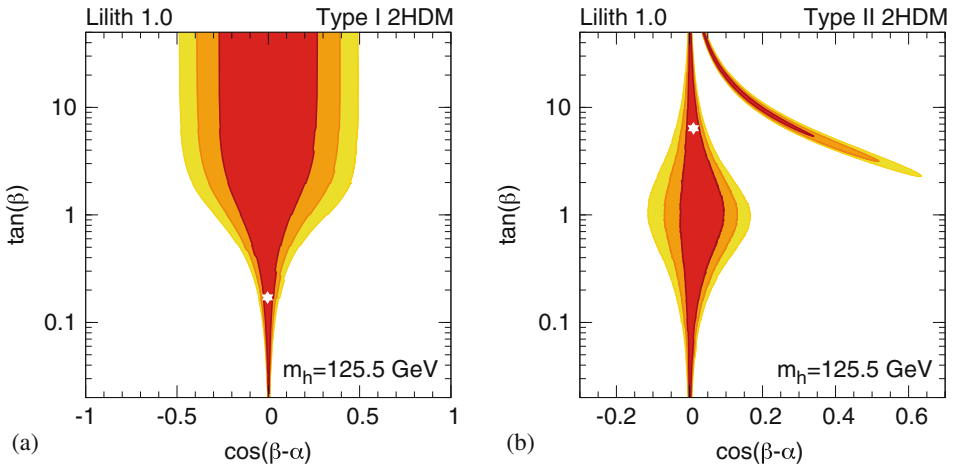

Figure 1. The red, orange and yellow regions represent the 68%, 95% and 99% CL allowed regions, respectively, coming from the Higgs signal strength measurements at the LHC. The (**a**) ((**b**)) panel shows the situation for Type I (II) model. The star-marked points correspond to the best-fit values (figures adapted from [23]).

3. Stability constraints

To discuss the stability of the potential, it is convenient to work with the notation of eq. (2). Here we derive the constraints on parameters β_i such that the scalar potential V is bounded from below in any direction in the field space [32,33]. It is sufficient to examine the quartic terms of the scalar potential (which we denote by V_4) because only this part of the potential will be dominant for large values of the field components of Φ_1 and Φ_2. We define $a \equiv \Phi_1^\dagger \Phi_1$, $b \equiv \Phi_2^\dagger \Phi_2$, $c \equiv \mathrm{Re}\, \Phi_1^\dagger \Phi_2$, $d \equiv \mathrm{Im}\, \Phi_1^\dagger \Phi_2$ and note that

$$ab \geq c^2 + d^2. \tag{21}$$

Using these definitions we can rewrite the quartic part of the scalar potential as follows [34]:

$$\begin{aligned} V_4 = {} & \frac{1}{2}(\sqrt{\beta_1}a - \sqrt{\beta_2}b)^2 + (\beta_3 + \sqrt{\beta_1\beta_2}) \\ & \times (ab - c^2 - d^2) + 2(\beta_3 + \beta_4 + \sqrt{\beta_1\beta_2})c^2 \\ & + (\mathrm{Re}\,\beta_5 - \beta_3 - \beta_4 - \sqrt{\beta_1\beta_2})(c^2 - d^2) \\ & - 2cd\,\mathrm{Im}\,\beta_5. \end{aligned} \tag{22}$$

Although we assume all the potential parameters to be real for our phenomenological studies, our arguments on stability do not depend on whether β_5 is real or complex. We must ensure that V_4 never becomes infinitely negative in any direction of the field space, i.e., for any choice of eight independent field parameters (four of Φ_1 and four of Φ_2). As Φ_1 and Φ_2 are two-component column matrices, it is possible to choose arbitrary non-zero values for a and b even when we make $c = d = 0$. But if a and/or b becomes zero, then $c = d = 0$ automatically. Keeping these in mind, we now proceed to find the stability constraints, i.e. the conditions under which the potential is bounded from below [32].

(i) Consider the field direction $b = 0$ (and therefore $c = d = 0$) and $a \to \infty$; then $V_4 = (\beta_1/2)a^2$. So, V_4 is not largely negative requires

$$\beta_1 \geq 0\,. \tag{23}$$

(ii) Consider the field direction $a = 0$ (and therefore $c = d = 0$) and $b \to \infty$; then $V_4 = (\beta_2/2)b^2$. So, V_4 is not largely negative requires

$$\beta_2 \geq 0\,. \tag{24}$$

(iii) Consider the field direction along which $a = \sqrt{\beta_2/\beta_1}b$ (so that the first term in eq. (22) vanishes) and $c = d = 0$. In addition to this we go to large field values in that direction, i.e., $a, b \to \infty$. Then, $V_4 = (\beta_3 + \sqrt{\beta_1\beta_2})ab$. Now, as $a, b > 0$ by definition, the condition for the potential not to hit $(-\infty)$ becomes

$$\beta_3 + \sqrt{\beta_1\beta_2} \geq 0. \tag{25}$$

(iv) Again consider the field direction in which $a = \sqrt{\beta_2/\beta_1}b$ along with $ab = c^2 + d^2$. Along this direction, V_4 is of the form

$$V_4 = Pc^2 + 2Qcd + Rd^2, \tag{26a}$$

where

$$P = \mathrm{Re}\,\beta_5 + \Lambda, \tag{26b}$$

$$Q = -\mathrm{Im}\,\beta_5, \tag{26c}$$

$$R = -\mathrm{Re}\,\beta_5 + \Lambda, \tag{26d}$$

with

$$S = \beta_3 + \beta_4 + \sqrt{\beta_1\beta_2}\,. \tag{26e}$$

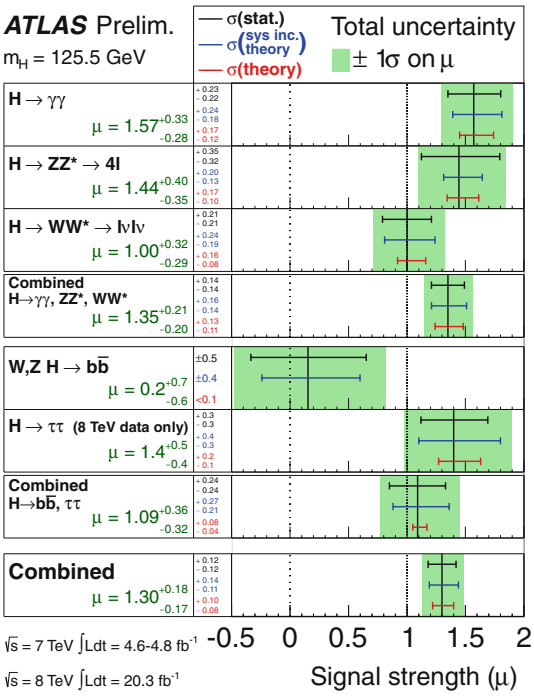

(a)

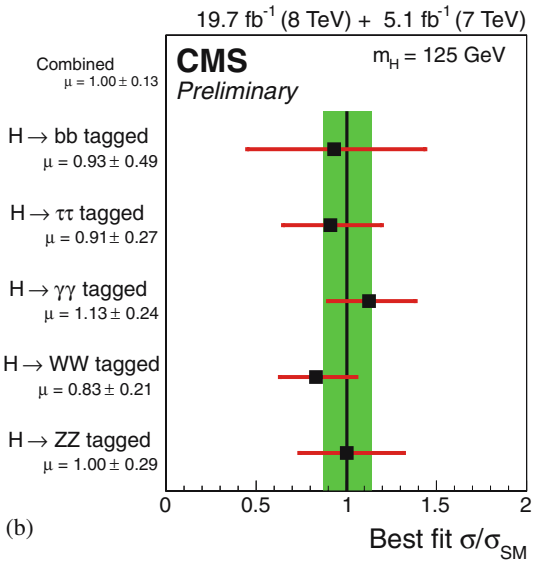

(b)

Figure 2. Current measurements of the Higgs signal strengths into different channels by the (**a**) ATLAS [30] and (**b**) CMS [31] Collaborations.

As c and d are still arbitrary, by choosing $d = 0$, $c \to \infty$ and $c = 0$, $d \to \infty$ successively, we require

$$P = \mathrm{Re}\,\beta_5 + S \geq 0, \tag{27a}$$

$$R = -\mathrm{Re}\,\beta_5 + S \geq 0, \tag{27b}$$

and hence

$$S \geq 0. \tag{27c}$$

To have another condition, let us recast eq. (26a) into the following form:

$$V_4 = P\left(c + \frac{Q}{P}d\right)^2 + \left(R - \frac{Q^2}{P}\right)d^2. \tag{28}$$

We can now choose a direction along which $c = -Q/Pd$ with $d \to \infty$ so that we have the following condition:

$$R - \frac{Q^2}{P} > 0 \Rightarrow PR > Q^2. \tag{29}$$

For the last step, remember that $P > 0$ (eq. (27a)) so that we can multiply both sides by P without flipping the inequality sign. After substituting for P, Q and R we get from eq. (29):

$$S^2 - (\mathrm{Re}\,\beta_5)^2 > (\mathrm{Im}\,\beta_5)^2 \Rightarrow S^2 > |\beta_5|^2\,, \tag{30a}$$

$$S > |\beta_5|\,, \tag{30b}$$

where, in the last step we have used the fact that $S > 0$ (eq. (27c)). As $|\beta_5| > \pm\beta_5,\ 0$, eq. (30b) puts a stronger constraint on S than eq. (27). Therefore, substituting for S, eq. (30b) becomes

$$\beta_3 + \beta_4 + \sqrt{\beta_1\beta_2} > |\beta_5|\,. \tag{31}$$

We now collect eqs (23)–(25) and (31) together and, using eq. (4), express them in terms of lambdas for later use:

$$\lambda_1 + \lambda_3 > 0\,, \tag{32a}$$

$$\lambda_2 + \lambda_3 > 0\,, \tag{32b}$$

$$(2\lambda_3 + \lambda_4) + 2\sqrt{(\lambda_1 + \lambda_3)(\lambda_2 + \lambda_3)} > 0, \tag{32c}$$

$$2\lambda_3 + \frac{\lambda_5 + \lambda_6}{2} - \frac{|\lambda_5 - \lambda_6|}{2} + 2\sqrt{(\lambda_1 + \lambda_3)(\lambda_2 + \lambda_3)} > 0. \tag{32d}$$

These conditions are both necessary and sufficient for ensuring stability of the electroweak vacuum. This has also been shown through rigorous analysis in [35,36]. In addition to these stability conditions, one also needs to ensure the positivity of the physical scalar masses [33,37]. Additionally, one might also wish to ensure

that the minimum is indeed the global minimum. The condition for the latter is given by [38]

$$m_{12}^2\left(m_{11}^2 - m_{22}^2\sqrt{\frac{\beta_1}{\beta_2}}\right)\left(\tan\beta - \sqrt[4]{\frac{\beta_1}{\beta_2}}\right) > 0. \qquad (33)$$

4. Unitarity constraints

In this section we study the energy growth of scattering amplitudes involving the scalar states. Any scattering amplitude can be expanded in terms of the partial waves as follows:

$$\mathcal{M}(\theta) = 16\pi\sum_{\ell=0}^{\infty} a_\ell(2\ell+1)P_\ell(\cos\theta), \qquad (34)$$

where θ is the scattering angle and $P_\ell(x)$ is the Legendre polynomial of order ℓ. The prescription is as follows: once we calculate the Feynman amplitude of a certain $2 \to 2$ scattering process, each of the partial wave amplitude (a_ℓ), in eq. (34), can be extracted by using the orthonormality of the Legendre polynomials. In the context of SM, the pioneering work has been done by Lee, Quigg and Thacker (LQT) [39]. They have analysed several two-body scatterings involving longitudinal gauge bosons and physical Higgs in the SM. All such scattering amplitudes are proportional to Higgs quartic coupling in the high energy limit. The $\ell = 0$ partial wave amplitude (a_0) is then extracted from these amplitudes and cast in the form of what is called an S-matrix having different two-body states as rows and columns. The largest eigenvalue of this matrix is bounded by the unitarity constraint, $|a_0| < 1$. This restricts the quartic Higgs self-coupling and therefore the Higgs mass to a maximum value.

The procedure has been extended to the case of a 2HDM scalar potential [40–44]. Here also same types of two-body scattering channels are considered. Thanks to the equivalence theorem [45,46], we can use unphysical Higgses instead of actual longitudinal components of the gauge bosons when considering the high-energy limit. The diagrams containing trilinear vertices will be suppressed by a factor of E^2 coming from the intermediate propagator. Thus, they do not contribute at high energies, and only the quartic couplings contribute. Since we are interested only in the eigenvalues of the S-matrix, we may, for convenience, proceed with the original fields of eq. (3) instead of the physical mass eigenstates.

To provide clarity, let us outline the method of obtaining the constraints. As already argued, only the dimensionless quartic couplings will contribute to the amplitudes at high energies. As a result, only $\ell = 0$ partial amplitude (a_0) will receive nonzero contribution from the leading-order terms in the scattering amplitudes. The task is to find the expressions of a_0 for every possible $2 \to 2$ scattering process and cast them in the form of an S-matrix which is constructed by taking the different two-body channels as rows and columns. Unitarity will restrict the magnitude of each of the eigenvalues of this S-matrix to lie below unity.

First, we identify all the possible two-particle channels. These two-particle states are made of the fields $w_k^\pm$, h_k and z_k corresponding to the parametrization of eq. (5). For our calculation, we consider neutral combinations out of the two-particle states (e.g., $w_i^+ w_j^-$, $h_i h_j$, $z_i z_j$, $h_i z_j$) and singly-charged two-particle states (e.g., $w_i^+ h_j$, $w_i^+ z_j$). In general, if we have n-number of doublets ϕ_k ($k = 1, \ldots, n$) in nHDM scenarios, there will be $(3n^2+n)$-number of neutral and $2n^2$-number of charged two-particle states. Clearly, the dimensions of S-matrices formed out of these two-particle states will be $(3n^2+n)\times(3n^2+n)$ and $2n^2 \times 2n^2$ for the neutral and charged cases respectively. The eigenvalues of these matrices should be bounded by the unitarity constraint.

The neutral channel S-matrix for 2HDM is a 14×14 matrix with the following two-particle states as rows and columns:

$$w_1^+w_1^-,\ w_2^+w_2^-,\ w_1^+w_2^-,\ w_2^+w_1^-,\ \frac{h_1h_1}{\sqrt{2}}, \frac{z_1z_1}{\sqrt{2}}, \frac{h_2h_2}{\sqrt{2}},$$
$$\frac{z_2z_2}{\sqrt{2}}, h_1z_2,\ h_2z_1,\ z_1z_2,\ h_1h_2,\ h_1z_1,\ h_2z_2. \qquad (35)$$

The factor of $1/\sqrt{2}$ associated with the identical particle states arises due to Bose symmetry. In the most general case, finding the eigenvalues of the 14×14 matrix would be a tedious job. But the potential of eq. (3) contains some obvious symmetries in its quartic terms. These symmetries will allow us to decompose the full matrix in smaller blocks. Now, each term in the quartic part of the potential always contains even number of indices (1 or 2). Consequently, a state x_1y_1 or x_2y_2 will always scatter into x_1y_1 or x_2y_2 but not into x_1y_2 or x_2y_1 and vice versa. Furthermore, CP symmetry is conserved. This implies that a neutral combination h_ih_j or z_iz_j will never go into h_iz_j. Keeping these facts in mind we can now decompose the S-matrix in the neutral sector into smaller blocks as follows:

$$\mathcal{M}_N = \begin{pmatrix} (\mathcal{M}_N^{11})_{6\times6} & 0 & 0 \\ 0 & (\mathcal{M}_N^{11})_{2\times2} & 0 \\ 0 & 0 & (\mathcal{M}_N^{12})_{6\times6} \end{pmatrix}. \qquad (36)$$

The submatrices are given below:

$$(\mathcal{M}_N^{11})_{6\times6} = \begin{array}{c} \\ w_1^+w_1^- \\ w_2^+w_2^- \\ \frac{z_1z_1}{\sqrt{2}} \\ \frac{h_1h_1}{\sqrt{2}} \\ \frac{z_2z_2}{\sqrt{2}} \\ \frac{h_2h_2}{\sqrt{2}} \end{array} \begin{array}{c} \begin{array}{cccccc} w_1^+w_1^- & w_2^+w_2^- & \frac{z_1z_1}{\sqrt{2}} & \frac{h_1h_1}{\sqrt{2}} & \frac{z_2z_2}{\sqrt{2}} & \frac{h_2h_2}{\sqrt{2}} \end{array} \\ \begin{pmatrix} 4(\lambda_1+\lambda_3) & 2\lambda_3+\frac{\lambda_5+\lambda_6}{2} & \sqrt{2}(\lambda_1+\lambda_3) & \sqrt{2}(\lambda_1+\lambda_3) & \sqrt{2}\left(\lambda_3+\frac{\lambda_4}{2}\right) & \sqrt{2}\left(\lambda_3+\frac{\lambda_4}{2}\right) \\ 2\lambda_3+\frac{\lambda_5+\lambda_6}{2} & 4(\lambda_2+\lambda_3) & \sqrt{2}\left(\lambda_3+\frac{\lambda_4}{2}\right) & \sqrt{2}\left(\lambda_3+\frac{\lambda_4}{2}\right) & \sqrt{2}(\lambda_2+\lambda_3) & \sqrt{2}(\lambda_2+\lambda_3) \\ \sqrt{2}(\lambda_1+\lambda_3) & \sqrt{2}\left(\lambda_3+\frac{\lambda_4}{2}\right) & 3(\lambda_1+\lambda_3) & (\lambda_1+\lambda_3) & \lambda_3+\frac{\lambda_5}{2} & \lambda_3+\frac{\lambda_6}{2} \\ \sqrt{2}(\lambda_1+\lambda_3) & \sqrt{2}\left(\lambda_3+\frac{\lambda_4}{2}\right) & (\lambda_1+\lambda_3) & 3(\lambda_1+\lambda_3) & \lambda_3+\frac{\lambda_6}{2} & \lambda_3+\frac{\lambda_5}{2} \\ \sqrt{2}\left(\lambda_3+\frac{\lambda_4}{2}\right) & \sqrt{2}(\lambda_2+\lambda_3) & \lambda_3+\frac{\lambda_5}{2} & \lambda_3+\frac{\lambda_6}{2} & 3(\lambda_2+\lambda_3) & (\lambda_2+\lambda_3) \\ \sqrt{2}\left(\lambda_3+\frac{\lambda_4}{2}\right) & \sqrt{2}(\lambda_2+\lambda_3) & \lambda_3+\frac{\lambda_6}{2} & \lambda_3+\frac{\lambda_5}{2} & (\lambda_2+\lambda_3) & 3(\lambda_2+\lambda_3) \end{pmatrix} \end{array}, \tag{37a}$$

$$(\mathcal{M}_N^{11})_{2\times2} = \begin{array}{c} \\ h_1z_1 \\ h_2z_2 \end{array} \begin{array}{c} \begin{array}{cc} h_1z_1 & h_2z_2 \end{array} \\ \begin{pmatrix} 2(\lambda_1+\lambda_3) & \frac{\lambda_5-\lambda_6}{2} \\ \frac{\lambda_5-\lambda_6}{2} & 2(\lambda_2+\lambda_3) \end{pmatrix} \end{array}, \tag{37b}$$

$$(\mathcal{M}_N^{12})_{6\times6} = \begin{array}{c} \\ w_1^+w_2^- \\ w_2^+w_1^- \\ h_1z_2 \\ h_2z_1 \\ z_1z_2 \\ h_1h_2 \end{array} \begin{array}{c} \begin{array}{cccccc} w_1^+w_2^- & w_2^+w_1^- & h_1z_2 & h_2z_1 & z_1z_2 & h_1h_2 \end{array} \\ \begin{pmatrix} 2\lambda_3+\frac{\lambda_5+\lambda_6}{2} & \lambda_5-\lambda_6 & -\frac{i}{2}(\lambda_4-\lambda_6) & \frac{i}{2}(\lambda_4-\lambda_6) & \frac{\lambda_5-\lambda_4}{2} & \frac{\lambda_5-\lambda_4}{2} \\ \lambda_5-\lambda_6 & 2\lambda_3+\frac{\lambda_5+\lambda_6}{2} & \frac{i}{2}(\lambda_4-\lambda_6) & -\frac{i}{2}(\lambda_4-\lambda_6) & \frac{\lambda_5-\lambda_4}{2} & \frac{\lambda_5-\lambda_4}{2} \\ \frac{i}{2}(\lambda_4-\lambda_6) & -\frac{i}{2}(\lambda_4-\lambda_6) & 2\lambda_3+\lambda_6 & \frac{\lambda_5-\lambda_6}{2} & 0 & 0 \\ -\frac{i}{2}(\lambda_4-\lambda_6) & \frac{i}{2}(\lambda_4-\lambda_6) & \frac{\lambda_5-\lambda_6}{2} & 2\lambda_3+\lambda_6 & 0 & 0 \\ \frac{\lambda_5-\lambda_4}{2} & \frac{\lambda_5-\lambda_4}{2} & 0 & 0 & 2\lambda_3+\lambda_5 & \frac{\lambda_5-\lambda_6}{2} \\ \frac{\lambda_5-\lambda_4}{2} & \frac{\lambda_5-\lambda_4}{2} & 0 & 0 & \frac{\lambda_5-\lambda_6}{2} & 2\lambda_3+\lambda_5 \end{pmatrix} \end{array}. \tag{37c}$$

The same exercise can be repeated for the charged two-particle state combinations. With the singly charged state combinations, it will be a 8×8 matrix which will take the following block diagonal form:

$$\mathcal{M}_C = \begin{pmatrix} (\mathcal{M}_C^{11})_{4\times4} & 0 \\ 0 & (\mathcal{M}_C^{12})_{4\times4} \end{pmatrix}. \tag{38}$$

The submatrices are given below:

$$(\mathcal{M}_C^{11})_{4\times4} = \begin{array}{c} \\ h_1w_1^+ \\ h_2w_2^+ \\ z_1w_1^+ \\ z_2w_2^+ \end{array} \begin{array}{c} \begin{array}{cccc} h_1w_1^+ & h_2w_2^+ & z_1w_1^+ & z_2w_2^+ \end{array} \\ \begin{pmatrix} 2(\lambda_1+\lambda_3) & \frac{\lambda_5-\lambda_4}{2} & 0 & -\frac{i}{2}(\lambda_4-\lambda_6) \\ \frac{\lambda_5-\lambda_4}{2} & 2(\lambda_2+\lambda_3) & -\frac{i}{2}(\lambda_4-\lambda_6) & 0 \\ 0 & \frac{i}{2}(\lambda_4-\lambda_6) & 2(\lambda_1+\lambda_3) & \frac{\lambda_5-\lambda_4}{2} \\ \frac{i}{2}(\lambda_4-\lambda_6) & 0 & \frac{\lambda_5-\lambda_4}{2} & 2(\lambda_2+\lambda_3) \end{pmatrix} \end{array}, \tag{39a}$$

$$(\mathcal{M}_C^{12})_{4\times4} = \begin{array}{c} \\ h_1w_2^+ \\ h_2w_1^+ \\ z_1w_2^+ \\ z_2w_1^+ \end{array} \begin{array}{c} \begin{array}{cccc} h_1w_2^+ & h_2w_1^+ & z_1w_2^+ & z_2w_1^+ \end{array} \\ \begin{pmatrix} 2\lambda_3+\lambda_4 & \frac{\lambda_5-\lambda_4}{2} & 0 & \frac{i}{2}(\lambda_4-\lambda_6) \\ \frac{\lambda_5-\lambda_4}{2} & 2\lambda_3+\lambda_4 & \frac{i}{2}(\lambda_4-\lambda_6) & 0 \\ 0 & -\frac{i}{2}(\lambda_4-\lambda_6) & 2\lambda_3+\lambda_4 & \frac{\lambda_5-\lambda_4}{2} \\ -\frac{i}{2}(\lambda_4-\lambda_6) & 0 & \frac{\lambda_5-\lambda_4}{2} & 2\lambda_3+\lambda_4 \end{pmatrix} \end{array}. \tag{39b}$$

The eigenvalues for these matrices are given by

(a) $(\mathcal{M}_N^{11})_{6\times6}$: $a_1^\pm,\ a_2^\pm,\ a_3^\pm$.
(b) $(\mathcal{M}_N^{11})_{2\times2}$: $a_3^\pm$.
(c) $(\mathcal{M}_N^{12})_{6\times6}$: $b_1,\ b_2,\ b_3,\ b_4,\ b_5$, with b_5 two-fold degenerate.
(d) $(\mathcal{M}_C^{11})_{4\times4}$: $a_2^\pm,\ a_3^\pm$.
(e) $(\mathcal{M}_C^{12})_{4\times4}$: $b_2,\ b_4,\ b_5,\ b_6$.

We also display the explicit expressions for these eigenvalues:

$$a_1^\pm = 3(\lambda_1+\lambda_2+2\lambda_3) \pm\sqrt{9(\lambda_1-\lambda_2)^2+\left(4\lambda_3+\lambda_4+\frac{\lambda_5+\lambda_6}{2}\right)^2}, \quad (40a)$$

$$a_2^\pm = (\lambda_1+\lambda_2+2\lambda_3) \pm\sqrt{(\lambda_1-\lambda_2)^2+\frac{1}{4}(2\lambda_4-\lambda_5-\lambda_6)^2}, \quad (40b)$$

$$a_3^\pm = (\lambda_1+\lambda_2+2\lambda_3) \pm\sqrt{(\lambda_1-\lambda_2)^2+\frac{1}{4}(\lambda_5-\lambda_6)^2}, \quad (40c)$$

$$b_1 = 2\lambda_3-\lambda_4-\frac{1}{2}\lambda_5+\frac{5}{2}\lambda_6, \quad (40d)$$

$$b_2 = 2\lambda_3+\lambda_4-\frac{1}{2}\lambda_5+\frac{1}{2}\lambda_6, \quad (40e)$$

$$b_3 = 2\lambda_3-\lambda_4+\frac{5}{2}\lambda_5-\frac{1}{2}\lambda_6, \quad (40f)$$

$$b_4 = 2\lambda_3+\lambda_4+\frac{1}{2}\lambda_5-\frac{1}{2}\lambda_6, \quad (40g)$$

$$b_5 = 2\lambda_3+\frac{1}{2}\lambda_5+\frac{1}{2}\lambda_6, \quad (40h)$$

$$b_6 = 2(\lambda_3+\lambda_4)-\frac{1}{2}\lambda_5-\frac{1}{2}\lambda_6. \quad (40i)$$

Each of the above eigenvalues will be bounded from the unitarity constraint as

$$|a_i^\pm|,\ |b_i| \le 16\pi. \quad (41)$$

5. Numerical constraints on the scalar masses

We now investigate the implications of the above conditions on the physical scalar masses, especially the nonstandard ones. Figure 3 shows the region allowed by the combined constraints from unitarity and the boundedness of the potential for $\lambda_5 = 0$, i.e., exact Z_2 symmetry. Two noteworthy features emerge [47]:

(i) From figure 3a, one can read the upper and lower limits on $\tan\beta$ as $1/8 < \tan\beta < 8$.
(ii) The upper limits on nonstandard scalar masses are given by: $m_H,\ m_A,\ m_{H^+} < 1$ TeV.

To understand the origin of the above limits we look into the eigenvalues of eq. (40). The first two constraints for boundedness in eq. (32) can be combined into

$$\lambda_1+\lambda_2+2\lambda_3 > 0. \quad (42)$$

Together with the condition $|a_1^\pm| < 16\pi$, this implies

$$0 < \lambda_1+\lambda_2+2\lambda_3 < \frac{16\pi}{3}, \quad (43)$$

$$\Rightarrow 0 < \left(m_H^2-\frac{1}{2}\lambda_5 v^2\right)(\tan^2\beta+\cot^2\beta) + 2m_h^2 < \frac{32\pi v^2}{3}, \quad (44)$$

where the last expression is obtained from the previous one by using eq. (16) in the alignment limit. As the heavier CP-even Higgs mass $m_H > 125$ GeV, a limit on $\tan\beta$ (as well as $\cot\beta$) is obtained when $\lambda_5 = 0$. As the minimum value of $(\tan^2\beta+\cot^2\beta)$ is 2 when $\tan\beta = 1$, the maximum possible value of m_H is obtained for

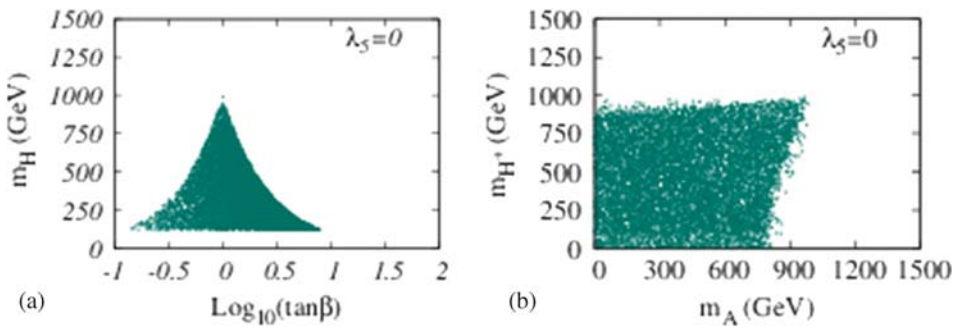

Figure 3. Allowed region (shown by scattered points) from unitarity and stability for exact Z_2 symmetry ($\lambda_5 = 0$).

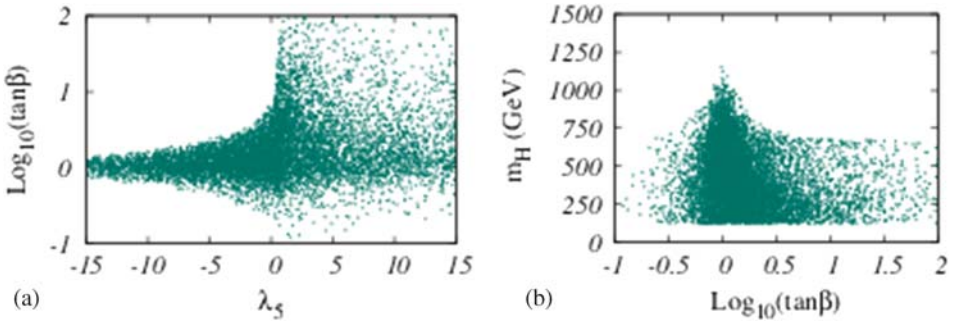

Figure 4. Relaxation of the constraints on $\tan\beta$ for nonzero λ_5. Figure 4b should be compared with figure 3a.

$\tan\beta = 1$. Equation (44) thus explains the $\tan\beta$-dependent bound on m_H as depicted in figure 3a.

To obtain restrictions on the individual masses, m_A and m_{H^+}, we use the following inequalities:

$$|b_1 - b_3| \equiv 3|\lambda_6 - \lambda_5| < 32\pi \Rightarrow \left| m_A^2 - \frac{1}{2}\lambda_5 v^2 \right| < \frac{16\pi v^2}{3}, \tag{45a}$$

$$|b_6 - b_3| \equiv 3|\lambda_4 - \lambda_5| < 32\pi \Rightarrow \left| m_{H^+}^2 - \frac{1}{2}\lambda_5 v^2 \right| < \frac{16\pi v^2}{3}. \tag{45b}$$

Using eqs (45a) and (45b) we put limits on m_A and m_{H^+}, respectively, when $\lambda_5 = 0$. Additionally, due to the inequality

$$|b_1 - b_6| \equiv 3|\lambda_6 - \lambda_4| < 32\pi \Rightarrow |m_A^2 - m_{H^+}^2| < \frac{16\pi v^2}{3}, \tag{46}$$

we expect the splitting between m_A and m_{H^+} to be always restricted. It is also interesting to note that the conclusions obtained from eqs (45a), (45b) and (46) do not depend on the imposition of the alignment condition.

From eq. (44) we also observe that the allowed space for $\tan\beta$ is further squeezed if $\lambda_5 < 0$, but the bound is relaxed if $\lambda_5 > 0$. This feature emerges from figure 4a. In addition to this, we can see from eq. (44) that m_H^2 must be close to $1/2\lambda_5 v^2$ if $\tan\beta$ moderately deviates from unity. This feature is reflected by the horizontal tail in figure 4b on both sides of the peak. The width of the tail is a result of the variation of λ_5 in the range $[-15, 15]$.

From eqs (45a), (45b) and (44) we note that the upper bounds on the nonstandard scalar masses will be

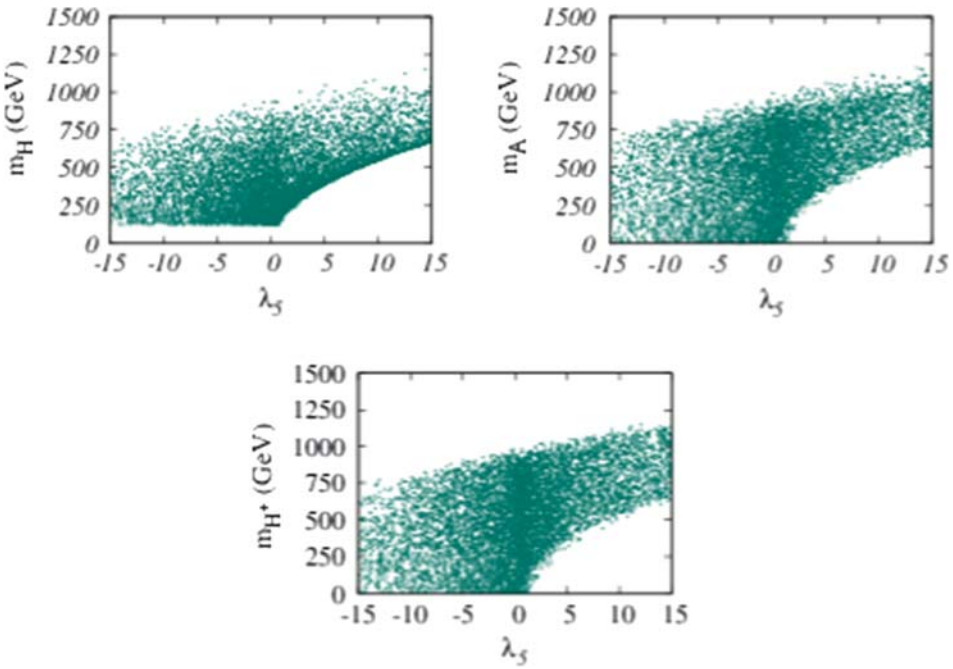

Figure 5. Effect of nonzero λ_5 on the constraints on the nonstandard masses.

relaxed for $\lambda_5 > 0$ and get tighter for $\lambda_5 < 0$. Figure 5 reflects these features.

An interesting alternative arises if instead of Z_2 one imposes a $U(1)$ symmetry under which $\Phi_1 \to \Phi_1$ and $\Phi_2 \to e^{i\alpha}\Phi_2$. This $U(1)$ symmetry needs to be softly broken to forbid the appearance of an exactly massless pseudoscalar. This $U(1)$ symmetry, in the quartic terms, implies $\beta_5 = 0$ in eq. (2) or $\lambda_5 = \lambda_6$ in eq. (3). The constraints on the scalar masses imposed by the stability and unitarity conditions in eqs (32) and (40) are plotted in figure 6 for $\tan\beta = 1$, 5 and 10 by performing random scan over all nonstandard scalar masses.

The following salient features emerge from the plots:

(i) There is a correlation between m_A and m_H which gets stronger for larger values of $\tan\beta$. They become nearly degenerate once $\tan\beta > 10$. To understand this, we observe that eq. (44) for $\lambda_5 = \lambda_6$ reduces to

$$0 \le (m_H^2 - m_A^2)(\tan^2\beta + \cot^2\beta) + 2m_h^2 \le \frac{32\pi v^2}{3}. \tag{47}$$

Clearly, for $\tan\beta$ away from unity, H and A are nearly degenerate.

(ii) There is a similar correlation between m_H and m_{H^+}, but unlike the previous point, without any dependence on $\tan\beta$. This can again be seen from the inequalities of eqs (45a) and (45b) keeping in mind that now $m_A^2 = (1/2)\lambda_5 v^2$.

(iii) The unitarity conditions essentially apply on the difference of the nonstandard squared masses. Any individual mass can be arbitrarily large without affecting the unitarity conditions. This conclusion crucially depends on the existence of a $U(1)$ symmetry and its soft breaking term in the potential. When the symmetry of the potential is only a discrete Z_2, considerations of unitarity do restrict the individual nonstandard masses as has already been shown.

(iv) The splitting between the heavy scalar masses is also constrained by the oblique electroweak T-parameter, whose expression in the decoupling limit is given by [50,51]

$$T = \frac{1}{16\pi \sin^2\theta_w M_W^2}[F(m_{H^+}^2, m_H^2) + F(m_{H^+}^2, m_A^2) - F(m_H^2, m_A^2)], \tag{48}$$

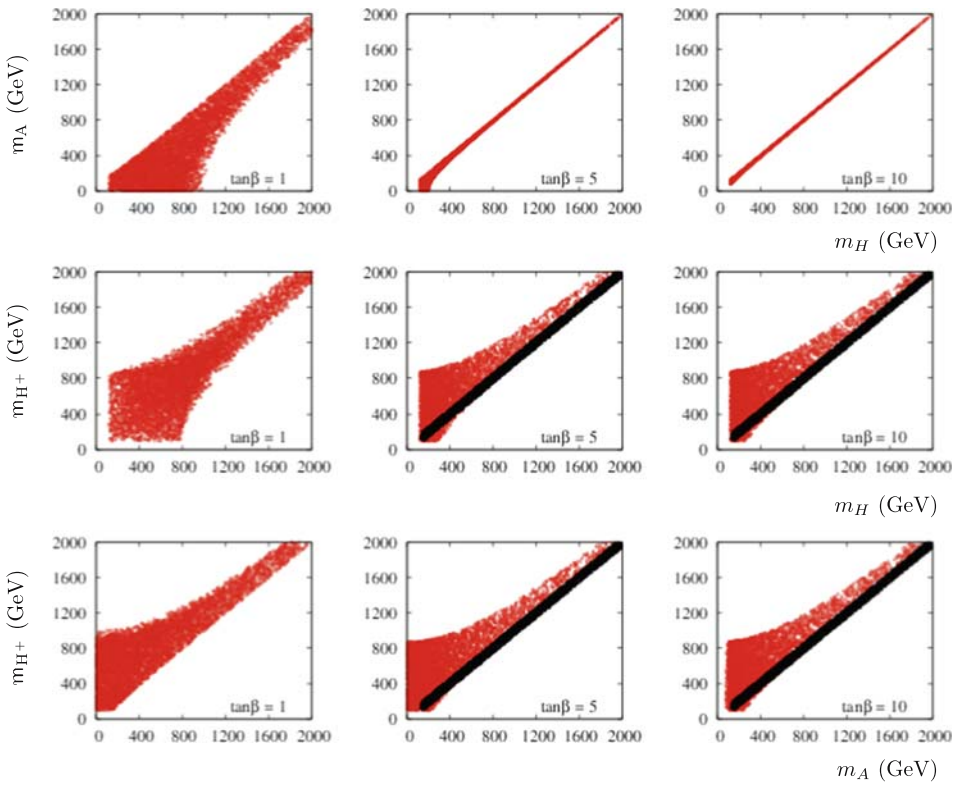

Figure 6. 2HDM potential with softly broken $U(1)$ symmetry: regions allowed in m_H–m_A, m_H–m_{H^+} and m_A–m_{H^+} planes from unitarity and stability (red points), and from T-parameter (black points), for three choices of $\tan\beta$. The plots have been taken from [48], where $m_{H^+} > 100$ GeV was assumed to respect LEP direct search bound [49].

with

$$F(x, y) = \frac{x+y}{2} - \frac{xy}{x-y} \ln(x/y). \quad (49)$$

The new physics part in the T-parameter is given by[52]

$$T = 0.05 \pm 0.12. \quad (50)$$

To provide intuition into the constraints from the T-parameter, we assume $m_H = m_A$, which is anyway dictated by the unitarity constraints for $\tan\beta$ somewhat away from unity. It then follows from eq. (48) that the splitting between m_{H^+} and m_H is approximately 50 GeV, for $|m_{H^+} - m_H| \ll m_{H^+}, m_H$. It follows from figure 6 that the constraints from the T-parameter are stronger than those from unitarity and stability.

On the other hand, for $\tan\beta = 1$, unitarity and stability do not compel m_H and m_A to be very close. Then, the T-parameter cannot give any definitive constraints in the planes of the nonstandard scalar masses, unlike the unitarity and stability constraints. For this reason, we have shown only the unitarity/stability constraints in figure 6 for $\tan\beta = 1$.

(v) For moderate or large $\tan\beta$, the unitarity and stability constraints together with the T-parameter constraints imply that all three heavy scalar states are nearly degenerate in the alignment limit.

For completeness, we also comment on the high-scale validity of 2HDMs [53]. After the Higgs discovery, it is well known that the SM perhaps needs to be augmented by new physics at energies beyond 10^8–10^{10} GeV [54,55]. The reason behind this is the following: the Higgs boson mass ∼125 GeV turns out to be a little 'smaller' than what could have made the SM ultraviolet safe up to Planck scale. More precisely, in the tussle between the top-Yukawa interaction (which tries to pull down the scalar quartic coupling) and the quartic self-interaction (which tries to push itself up) during the course of RG evolution, the top-Yukawa takes an upper hand and pulls the SM quartic coupling to negative values well below the Planck scale. One might expect the situation to improve in a 2HDM because of the presence of additional quartic couplings. But the 2HDM potential of eqs (2) and (3), without the soft-breaking term, still fails to maintain stability all the way up to the Planck scale [56–58]. Even in the presence of a soft-breaking parameter, in the alignment limit, a lower bound on $\tan\beta$ ($\gtrsim$3) [57,58] is obtained from the requirement that the effect of the top-Yukawa ($= \sqrt{2}m_t/(v\sin\beta)$ in 2HDM *vis-à-vis* $\sqrt{2}m_t/v$ in SM) is sufficiently diluted to maintain the required stability. Moreover, certain correlations between the nonstandard masses and the soft-breaking parameter need to be maintained.

6. Conclusions and outlook

Based on data on the new scalar resonance observed at the LHC, two important conclusions have been drawn: (i) its mass is approximately 125 GeV and (ii) its couplings to gauge bosons and fermions are similar to the SM Higgs boson. In the 2HDM framework, the latter observation pushes us to the alignment limit. Put these two conditions together, the 2HDM parameter space is more constrained than ever. Some important observations in this context are the following:

(a) When the potential has a global $U(1)$ symmetry, rather than a discrete Z_2, as well as a soft-breaking term, unitarity restricts the mass-squared differences of the nonstandard scalars. So the individual nonstandard masses, like m_H, m_A or m_{H^+}, can grow very large without necessarily violating unitarity.

(b) Strictly when both doublets receive VEVs and the potential has an exact discrete or a global continuous symmetry, the model exhibits features of nondecoupling. For example, observables do not necessarily reduce to their SM values even when nonstandard scalars are too heavy. In [59], we have demonstrated this behaviour in the context of $h \to \gamma\gamma$, where in the limit of an exact discrete symmetry, the Higgs signal strength in the diphoton channel at the LHC, given by $\mu_{\gamma\gamma}$, was shown to retain nonstandard effects even when the charged Higgs mass is pushed to extremely large values. Employing the soft-breaking term, it is possible to ensure decoupling. If the symmetry to start with is a discrete Z_2, one cannot avoid fine-tuning between the charged Higgs mass and the soft-breaking parameter to reach the decoupling limit. On the other hand, if the starting symmetry is a global $U(1)$, the soft-breaking parameter gets related to the pseudoscalar mass. In this case, the combined constraints from unitarity and the T-parameter naturally lead to the decoupling limit without any need for fine-tuning. For details, we refer the readers to ref. [59].

Acknowledgements

DD thanks the Department of Atomic Energy, India, for financial support.

References

[1] ATLAS Collaboration: G Aad *et al*, *Phys. Lett. B* **716**, 1 (2012), arXiv:1207.7214
[2] CMS Collaboration: S Chatrchyan *et al*, *Phys. Lett. B* **716**, 30 (2012), arXiv:1207.7235
[3] P W Higgs, *Phys. Rev. Lett.* **13**, 508 (1964)
[4] P W Higgs, *Phys. Rev.* **145**, 1156 (1966)
[5] F Englert and R Brout, *Phys. Rev. Lett.* **13**, 321 (1964)
[6] G Guralnik, C Hagen and T Kibble, *Phys. Rev. Lett.* **13**, 585 (1964)
[7] T Kibble, *Phys. Rev.* **155**, 1554 (1967)
[8] P Langacker, *Phys. Rep.* **72**, 185 (1981)
[9] Particle Data Group Collaboration: K Olive *et al*, *Chin. Phys. C* **38**, 090001 (2014)
[10] G Branco, P Ferreira, L Lavoura, M Rebelo, M Sher *et al*, *Phys. Rep.* **516**, 1 (2012), arXiv:1106.0034
[11] G Dorsch, S Huber and J No, *J. High Energy Phys.* **1310**, 029 (2013), arXiv:1305.6610
[12] S L Glashow and S Weinberg, *Phys. Rev. D* **15**, 1958 (1977)
[13] E Paschos, *Phys. Rev. D* **15**, 1966 (1977)
[14] A Pich and P Tuzon, *Phys. Rev. D* **80**, 091702 (2009), arXiv:0908.1554
[15] P Ferreira, L Lavoura and J P Silva, *Phys. Lett. B* **688**, 341 (2010), arXiv:1001.2561
[16] G Branco, W Grimus and L Lavoura, *Phys. Lett. B* **380**, 119 (1996), hep-ph/9601383
[17] G Bhattacharyya, D Das and A Kundu, *Phys. Rev. D* **89(9)**, 095029 (2014), arXiv:1402.0364
[18] F Botella, G Branco, A Carmona, M Nebot, L Pedro *et al*, *J. High Energy Phys.* **1407**, 078 (2014), arXiv:1401.6147
[19] A S Joshipura and S D Rindani, *Phys. Lett. B* **260**, 149 (1991)
[20] J F Gunion and H E Haber, *Phys. Rev. D* **72**, 095002 (2005), hep-ph/0506227
[21] P Ferreira, H E Haber and J P Silva, *Phys. Rev. D* **79**, 116004 (2009), arXiv:0902.1537
[22] P Ferreira, M Maniatis, O Nachtmann and J P Silva, *J. High Energy Phys.* **1008**, 125 (2010), arXiv:1004.3207
[23] J Bernon, B Dumont and S Kraml, arXiv:1409.1588
[24] B Coleppa, F Kling and S Su, *J. High Energy Phys.* **1401**, 161 (2014), arXiv:1305.0002
[25] O Eberhardt, U Nierste and M Wiebusch, *J. High Energy Phys.* **1307**, 118 (2013), arXiv:1305.1649
[26] C-Y Chen, S Dawson and M Sher, *Phys. Rev. D* **88**, 015018 (2013), arXiv:1305.1624
[27] N Craig, J Galloway and S Thomas, arXiv:1305.2424
[28] B Dumont, J F Gunion, Y Jiang and S Kraml, *Phys. Rev. D* **90**, 035021 (2014), arXiv:1405.3584
[29] P S B Dev and A Pilaftsis, arXiv:1503.09140
[30] ATLAS Collaboration: *ATLAS-CONF-2014-009*, https://atlas.web.cern.ch/Atlas/GROUPS/PHYSICS/CONFNOTES/ATLAS-CONF-2014-009/
[31] CMS Collaboration: *CMS-PAS-HIG-14-009*, http://cds.cern.ch/record/1728249?ln=en
[32] N G Deshpande and E Ma, *Phys. Rev. D* **18**, 2574 (1978)
[33] B M Kastening, hep-ph/9307224
[34] J F Gunion and H E Haber, *Phys. Rev. D* **67**, 075019 (2003), hep-ph/0207010
[35] K Klimenko, *Theor. Math. Phys.* **62**, 58 (1985)
[36] M Maniatis, A von Manteuffel, O Nachtmann and F Nagel, *Eur. Phys. J. C* **48**, 805 (2006), hep-ph/0605184
[37] S Nie and M Sher, *Phys. Lett. B* **449**, 89 (1999), hep-ph/9811234
[38] A Barroso, P Ferreira, I Ivanov and R Santos, *J. High Energy Phys.* **1306**, 045 (2013), arXiv:1303.5098
[39] B W Lee, C Quigg and H Thacker, *Phys. Rev. D* **16**, 1519 (1977)
[40] J Maalampi, J Sirkka and I Vilja, *Phys. Lett. B* **265**, 371 (1991)
[41] S Kanemura, T Kubota and E Takasugi, *Phys. Lett. B* **313**, 155 (1993), hep-ph/9303263
[42] A G Akeroyd, A Arhrib and E-M Naimi, *Phys. Lett. B* **490**, 119 (2000), hep-ph/0006035
[43] J Horejsi and M Kladiva, *Eur. Phys. J. C* **46**, 81 (2006), hep-ph/0510154
[44] B Świeżewska, *Phys. Rev. D* **88(5)**, 055027 (2013), arXiv:1209.5725
[45] P B Pal, hep-ph/9405362
[46] J Horejsi, *Czech. J. Phys.* **47**, 951 (1997), hep-ph/9603321
[47] D Das, arXiv:1501.02610
[48] G Bhattacharyya, D Das, P B Pal and M Rebelo, *J. High Energy Phys.* **1310**, 081 (2013), arXiv:1308.4297
[49] LEP Higgs Working Group for Higgs boson searches, ALEPH, DELPHI, L3 and OPAL Collaboration: *Search for charged Higgs bosons: Preliminary combined results using LEP data collected at energies up to 209-GeV*, hep-ex/0107031
[50] H-J He, N Polonsky and S-f Su, *Phys. Rev. D* **64**, 053004 (2001), hep-ph/0102144
[51] W Grimus, L Lavoura, O Ogreid and P Osland, *J. Phys. G* **35**, 075001 (2008), arXiv:0711.4022
[52] M Baak and R Kogler, arXiv:1306.0571
[53] P Ferreira and D Jones, *J. High Energy Phys.* **0908**, 069 (2009), arXiv:0903.2856
[54] F Bezrukov, M Y Kalmykov, B A Kniehl and M Shaposhnikov, *J. High Energy Phys.* **1210**, 140 (2012), arXiv:1205.2893
[55] G Degrassi, S Di Vita, J Elias-Miro, J R Espinosa, G F Giudice *et al*, *J. High Energy Phys.* **1208**, 098 (2012), arXiv:1205.6497
[56] N Chakrabarty, U K Dey and B Mukhopadhyaya, *J. High Energy Phys.* **1412**, 166 (2014), arXiv:1407.2145
[57] D Das and I Saha, arXiv:1503.02135
[58] D Chowdhury and O Eberhardt, arXiv:1503.08216
[59] G Bhattacharyya and D Das, *Phys. Rev. D* **91**, 015005 (2015), arXiv:1408.6133